Studies on quark-mass dependence of the $N^*(920)$ pole from unitarized πN χPT amplitudes*

Xu Wang (王旭)[1†] Kai-Ge Kang (康凯歌)[1,2‡] Qu-Zhi Li (李衢智)[2§]
Zhiguang Xiao (肖志广)[2§] Han-Qing Zheng (郑汉青)[2#]

[1]School of Physics, Peking University, Beijing 100871, China
[2]Institute of Particle and Nuclear Physics, College of Physics, Sichuan University, Chengdu, Sichuan 610065, China

Abstract: The quark-mass dependence of the $N^*(920)$ pole is analyzed using K-matrix method, with the πN scattering amplitude calculated up to $O(p^3)$ order in chiral perturbation theory. As the quark mass increases, the $N^*(920)$ pole gradually approaches the real axis in the complex w-plane (where $w=\sqrt{s}$). Eventually, in the $O(p^2)$ case, it crosses the u-cut on the real axis and enters the adjacent Riemann sheet when the pion mass reaches 526 MeV. At order $O(p^3)$, the rate at which it approaches the real axis slows down; however, it remains uncertain whether it will ultimately cross the u-cut and enter the adjacent Riemann sheet. Additionally, the trajectory of the $N^*(920)$ pole is in qualitative agreement with the results from the linear σ model calculation.

Keywords: pion-nucleon scattering, chiral perturbation theory, sub-threshold resonance

DOI: **CSTR:**

I. INTRODUCTION

The study of pion-nucleon scattering has a history spanning over sixty years. It is therefore surprising that the pole structure of the sub-threshold $\pi-N$ scattering amplitude, particularly in the S_{11} channel, has only been clarified very recently. Two key findings have emerged: first, as demonstrated in Ref. [1], partial-wave amplitudes (PWAs) indeed contain poles — specifically, virtual states — located on the real axis below threshold on the second Riemann sheet (RSII). Second, a novel resonance pole has been identified in the S_{11} channel through various unitarized approaches, including the product representation [2−4], the K-matrix fit [5], and the N/D method [6]. The resonance pole is necessary mainly because the contribution of the left-hand cut to the phase shift is negative and the pole is required to compensate the left-hand cut to reproduce the experimental phase shift [3, 4]. The existence of this resonance has finally been confirmed by the *model-independent* Roy-Steiner equation formalism [7, 8], which respects analyticity, unitarity, and crossing symmetry of the S-matrix. This sub-threshold pole, located at $\sqrt{s}=(918\pm3)-i(163\pm9)$ MeV, has been designated as $N^*(920)$. See [9, 10] for recent reviews.

Meanwhile, understanding the quark-mass dependence of resonance poles is crucial, which offers a unique perspective on strong interaction physics. Lattice QCD provides a first-principle, non-perturbative framework to investigate how hadron states depend on the quark mass. However, parameterizations of infinite-volume PWAs can introduce model dependence when fitting finite-volume spectra using the Lüscher formula [11] and its generalizations [12−14]. Ref. [15] demonstrated a model-independent approach to interpreting lattice data via the generalized Roy equation, revealing that the σ meson becomes a bound state, with a new resonance emerging, at $m_\pi\simeq391$MeV. Similar studies have also been completed for πK scattering, as detailed in Refs. [16, 17]. Subsequently, the trajectory of the σ with varying m_π was illustrated within the $O(N)$ linear σ model (LσM) [18, 19].

The first attempt to trace the trajectory of the $N^*(920)$ with varying pion masses was conducted within the LσM

Received 12 December 2025; Accepted 25 February 2026

* This work is supported by China National Natural Science Foundation under Contract No. 12335002, 12375078. This work is also supported by "the Fundamental Research Funds for the Central Universities"

† E-mail: wangxu0604@stu.pku.edu.cn
‡ E-mail: kaige@alumni.pku.edu.cn
§ E-mail: liqz@scu.edu.cn (corresponding author)
ǂ E-mail: xiaozg@scu.edu.cn (corresponding author)
E-mail: zhenghq@scu.edu.cn

with nucleons [20]. In that renormalizable model, the authors simultaneously computed the trajectories of both the σ and the $N^*(920)$ using several unitarization methods at the one-loop level. The trajectory of the σ was found to be consistent with previous results, while that of the $N^*(920)$ was novel: it crosses the u-cut (the cut (c_L, c_R) in Fig. 1) to the adjacent Riemann sheet at tree level, disappearing from the RSII, yet remains on the complex plane of the RSII at the one-loop level.

To further elucidate the fate of the $N^*(920)$, this work employs Baryon Chiral Perturbation Theory (BχPT) to investigate its trajectory as the pion mass increases. As a low-energy effective field theory of QCD, BχPT has been successfully applied to describe πN elastic scattering phase shifts and the pion-nucleon σ-term. A particular advantage of BχPT in studies with unphysical pion masses is that other parameters, such as the nucleon mass m_N, pion decay constant F_π and the axial coupling constant g_A, can be determined self-consistently once the low-energy constants are fixed at the physical pion mass. The $\Delta(1232)$ state would not be explicitly included because it appears in P_{33} channel and will affect S_{11} only through crossed channel effect and the higher order loop effect. Thus, it is expected that its contribution will be small.

The paper is organized as follows. Section II gives a brief introduction to BχPT and PWAs of πN scatterings. In section III, the trajectory of $N^*(920)$ is presented at $O(p^2)$ and $O(p^3)$ orders for different sets of LECs values. We conclude with a brief summary in section IV.

II. A BRIEF INTRODUCTION TO BχPT AND PWAs OF πN SCATTERINGS

The Lagrangian in BχPT can be expanded as $\mathcal{L} = \sum_{i=1}^{\infty} \mathcal{L}_{\pi\pi}^{(2i)} + \sum_{j=1}^{\infty} \mathcal{L}_{\pi N}^{(j)}$, where the magnitudes of $\mathcal{L}_{\pi\pi}^{(2i)}$ and $\mathcal{L}_{\pi N}^{(j)}$ are $O(p^{2i})$ and $O(p^j)$, respectively. Terms of the meson part for calculation up to $O(p^4)$ are [21]

$$\mathcal{L}_{\pi\pi}^{(2)} = \frac{F^2}{4}\mathrm{Tr}\left[\nabla_\mu U (\nabla^\mu U)^\dagger\right] + \frac{F^2}{4}\mathrm{Tr}\left[\chi U^\dagger + U\chi^\dagger\right], \tag{1}$$

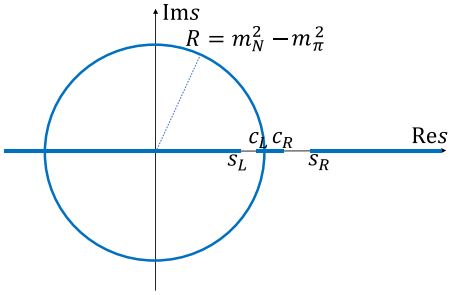

Fig. 1. (color online) Cuts in πN PWAs, represented by the bold lines. $s_L = (m_N - m_\pi)^2, c_L = (m_N^2 - m_\pi^2)^2/m_N^2, c_R = m_N^2 + 2m_\pi^2, s_R = (m_N + m_\pi)^2$

$$\begin{aligned}\mathcal{L}_{\pi\pi}^{(4)} = &\frac{l_3 + l_4}{16}\left[\mathrm{Tr}\left(\chi U^\dagger + U\chi^\dagger\right)\right]^2 \\ &+ \frac{l_4}{8}\mathrm{Tr}\left[\nabla_\mu U (\nabla^\mu U)^\dagger\right]\mathrm{Tr}\left(\chi U^\dagger + U\chi^\dagger\right),\end{aligned} \tag{2}$$

where F is the pion decay constant in the chiral limit. $\chi = M^2$ (assuming isospin symmetry) and M is the lowest order pion mass. Pions are contained in the SU(2) matrix:

$$U = \exp\left(i\frac{\phi}{F}\right), \quad \phi = \vec{\phi}\cdot\vec{\tau} = \begin{pmatrix} \pi_0 & \sqrt{2}\pi^+ \\ \sqrt{2}\pi^- & -\pi_0 \end{pmatrix}, \tag{3}$$

The covariant derivative acting on the pion fields is defined as $\nabla_\mu U = \partial_\mu U - ir_\mu U + iUl_\mu$, where l_μ and r_μ are the external fields.

The required baryon Lagrangians for calculation up to $O(p^3)$ are [22]

$$\mathcal{L}_{\pi N}^{(1)} = \bar{\Psi}\left\{i\not{D} - m + \frac{g}{2}\not{\gamma}\gamma_5 u_\mu\right\}\Psi, \tag{4}$$

$$\begin{aligned}\mathcal{L}_{\pi N}^{(2)} = \bar{\Psi}\Big\{&c_1\,\mathrm{Tr}[\chi_+] - \frac{c_2}{4m^2}\mathrm{Tr}[u_\mu u_\mu](D^\mu D^\mu + \mathrm{h.c.}) \\ &+ \frac{c_3}{2}\mathrm{Tr}[u^\mu u_\mu] - \frac{c_4}{4}\not{\gamma}\gamma^\mu[u_\mu, u_u]\Big\}\Psi,\end{aligned} \tag{5}$$

$$\begin{aligned}\mathcal{L}_{\pi N}^{(3)} = \bar{\Psi}\Big\{&-\frac{d_1 + d_2}{4m}\left([u_\mu, [D_u, u^\mu] + [D^\mu, u_u]]D^\mu + \mathrm{h.c.}\right) \\ &+ \frac{d_3}{12m^3}\left([u_\mu, [D_u, u_\lambda]]\left(D^\mu D^u D^\lambda + \mathrm{sym.}\right) + \mathrm{h.c.}\right) \\ &+ i\frac{d_5}{2m}\left([\chi_-, u_\mu]D^\mu + \mathrm{h.c.}\right) \\ &+ i\frac{d_{14} - d_{15}}{8m}\left(\sigma^{\mu u}\mathrm{Tr}\left[[D_\lambda, u_\mu]u_u - u_\mu[D_u, u_\lambda]\right]D^\lambda + \mathrm{h.c.}\right) \\ &+ \frac{d_{16}}{2}\not{\gamma}\gamma^5\mathrm{Tr}\left[\chi_+\right]u_\mu + \frac{id_{18}}{2}\not{\gamma}\gamma^5\left[D_\mu, \chi_-\right]\Big\}\Psi,\end{aligned} \tag{6}$$

where m and g are the bare nucleon mass and the bare axial-vector coupling constant, respectively. Those l_i, c_i and d_i are the LECs. The chiral vielbein and the covariant derivative with respect to the nucleon field are defined as

$$u_\mu = i\left[u^\dagger\left(\partial_\mu - ir_\mu\right)u - u\left(\partial_\mu - il_\mu\right)u^\dagger\right], \tag{7}$$

$$D_\mu = \partial_\mu + \Gamma_\mu, \tag{8}$$

$$\Gamma_\mu = \frac{1}{2}\left[u^\dagger\left(\partial_\mu - ir_\mu\right)u + u\left(\partial_\mu - il_\mu\right)u^\dagger\right], \tag{9}$$

$$u = \sqrt{U} = \exp\left(\frac{i\phi}{2F}\right). \tag{10}$$

According to the power counting rule [23], the amplitude for a diagram with L loops, I_ϕ inner pion lines, I_N inner nucleon lines and $N^{(k)}$ vertices from $O(p^k)$ Lagrangian are of $O(p^D)$, where

$$D = 4L - 2I_\phi - I_N + \sum_k^\infty kN^{(k)}.$$

In this manuscript, the full amplitudes of πN scatterings are calculated up to $O(p^3)$ order.

For the process $\pi^a(p) + N_i(q) \to \pi^{a'}(p') + N_f(q')$, the isospin amplitude can be decomposed as:

$$T = \chi_f^\dagger\left(\delta^{aa'}T^+ + \frac{1}{2}\left[\tau^{a'},\tau^a\right]T^-\right)\chi_i, \tag{11}$$

where τ^a $(a = 1,2,3)$ are Pauli matrices, and χ_i (χ_f) corresponds to the isospin wave function of the initial (final) nucleon state. The amplitudes with isospins $I = 1/2, 3/2$ can be written as

$$T^{I=1/2} = T^+ + 2T^-, \quad T^{I=3/2} = T^+ - T^-. \tag{12}$$

As for Lorentz structure, for an isospin index $I = 1/2, 3/2$,

$$T^I = \bar{u}^{(s')}(q')\left[A^I(s,t) + \frac{1}{2}\left(\not{p} + \not{p}'\right)B^I(s,t)\right]u^{(s)}(q), \tag{13}$$

with the superscripts $(s),(s')$ denoting the spins of Dirac spinors and three Mandelstam variables $s = (p+q)^2$, $t = (p-p'), u = (p-q')$ obeying the constraint $s+t+u = 2m_N^2 + 2m_\pi^2$. The partial wave amplitude $T_\pm^{I,J}$ for the L_{2I2J} channel with orbital angular momentum L, total angular momentum J and total isospin I is defined as:

$$T_\pm^{I,J} = T(L_{2I2J}) = T_{++}^{I,J}(s) \pm T_{+-}^{I,J}(s), \quad L = J \mp \frac{1}{2}, \tag{14}$$

where the definition of partial wave helicity amplitudes are written as:

$$\begin{aligned} T_{++}^{I,J} &= 2m_N A_C^{I,J}(s) + \left(s - m_\pi^2 - m_N^2\right)B_C^{I,J}(s) \\ T_{+-}^{I,J} &= -\frac{1}{\sqrt{s}}\Big[\left(s - m_\pi^2 + m_N^2\right)A_S^{I,J}(s) \\ &\quad + m_N\left(s + m_\pi^2 - m_N^2\right)B_S^{I,J}(s)\Big] \end{aligned} \tag{15}$$

with

$$F_{C/S}^{I,J}(s) = \int_{-1}^{1} \mathrm{d}z_s F^I(s,t)\left[P_{J+1/2}(z_s) \pm P_{J-1/2}(z_s)\right], \quad F = A, B \tag{16}$$

and $z_s = \cos\theta$ with θ the scattering angle. The partial wave amplitudes $T_\pm^{I,J}$ satisfy unitarity condition:

$$\mathrm{Im}\, T_\pm^{I,J}(s) = \rho(s, m_\pi, m_N)|T_\pm^{I,J}(s)|^2, \quad s > s_R = (m_\pi + m_N)^2. \tag{17}$$

For simplicity, we denote the PWA $T(S_{11})$ as T in the following.

The partial wave S matrix element in S_{11} channel can be defined as

$$S = 1 + 2i\rho(s)T, \tag{18}$$

where $\rho(s) = \sqrt{[s-(m_N+m_\pi)^2][s-(m_N-m_\pi)^2]}/s$. A K-matrix approximation is used to restore unitarity from perturbation amplitudes. Then, the partial wave amplitude and partial wave S matrix element are expressed as

$$\tilde{T} = \frac{K}{1 - i\rho K}, \ \tilde{S} = \frac{1 + i\rho K}{1 - i\rho K}, \tag{19}$$

where K needs to be real in the physical region above the πN threshold to meet the unitary requirement of the S matrix. Usually K is taken as the real part of the perturbation amplitude. For πN scattering, it is

$$\mathcal{K}^{(2)} \equiv T^{(2)} \tag{20}$$

for $O(p^2)$ calculation, while $\mathcal{K}^{(3)}$ is set to

$$T^{(3)} - i\rho(T^{(1)})^2 \tag{21}$$

for $O(p^3)$ calculation, because $T^{(3)}$ contains an imaginary part on the right hand cut [24].

The partial wave amplitude as constructed is a real analytic function on the complex s plane. There exists a physical cut, or right-hand cut, above the threshold $s > (m_N + m_\pi)^2$. Partial wave projection and loop integrals also introduce other cuts, called left-hand cuts. All the cut structures in πN scattering are shown in Fig. 1 [25, 26]. However, in general, such unitarization approximations suffer from problems of violation of analyticity and crossing symmetry [27−30].[1)] A direct consequence is the appearance of spurious physical sheet resonances (SPSRs). A case by case analysis seems to be required, at least, to ensure that the SPSRs play a minor contribution

1) For example, a [1,1] Padé approximant of $\pi\pi$ scattering tend to put all contributions from different sources, e.g., s channel poles, left hand cuts, crossed channel resonance exchanges, into one single s channel resonance.

to physical quantities such as phase shifts. Barring for this, the K-matrix unitarization provides a quick but rough estimates of the physical pole position such as $N^*(920)$.

III. ANALYSIS OF THE $N^*(920)$ POLE TRAJECTORY AND ITS QUARK MASS DEPENDENCE

To proceed, we follow Refs. [3, 24]. First, we repeat the $O(p^2)$ and $O(p^3)$ results of Ref. [24]. The obtained partial wave unitary amplitude can then be used to calculate the corresponding phase shift $\delta = \arctan[\rho\tilde{T}]$ and a subsequent fit to the phase shift data in turn determines the low energy constants. For the $O(p^2)$ calculations, we directly use the results in Ref. [3]:

$$c_1 = -0.841\ \text{GeV}^{-1},\ c_2 = 1.170\ \text{GeV}^{-1},$$
$$c_3 = -2.618\ \text{GeV}^{-1},\ c_4 = 1.677\ \text{GeV}^{-1}\ . \tag{22}$$

By substituting these low energy constants and physical quantities $m_N = 0.9383\ \text{GeV}, m_\pi = 0.1396\ \text{GeV}, F_\pi = 0.0924\ \text{GeV}, g_A = 1.267$, we can calculate the cuts and poles of the partial wave unitary matrix element of the S_{11} channel on the complex s plane. The pole corresponding to $N^*(920)$ resonance is found at $\sqrt{s} = 0.954 \pm i0.265\ \text{GeV}$.

In the isospin limit, the pion mass is related to the quark mass by the relation $m_\pi^2 \propto 2B_0\hat{m}$, where $\hat{m} = (m_u + m_d)/2$ [31]. Consequently, investigating the quark-mass dependence of the $N^*(920)$ resonance is equivalent to studying its evolution with increasing pion mass. Since by definition the effective Lagrangian is an expansion with respect to m_π and soft momentum p, the low energy constants l_i and d_i are m_π independent. The renormalization scheme is also chosen to be m_π independent, and thus the renormalized LECs are independent of m_π. Additionally, since key physical quantities (e.g., m_N, g_A, and F_π) are renormalized, it is essential to determine their values at different pion masses. Fortunately, within the framework of BχPT, these dependence relations can be directly computed. Up to the $O(p^3)$ order (one-loop diagrams), the explicit dependence relations are given by (this result can also be found in [32−35]) :

$$\begin{aligned}
&m_N = m - 4c_1M^2 + \Delta_m, \quad \Delta_m = \frac{3g^2 m_N}{32\pi^2F^2}\left[A_0(m_N^2) + M^2B_0(m_N^2, M^2, m_N^2)\right],\\
&F_\pi = F\left(1 + l_4^r\frac{M^2}{F^2} - \frac{1}{16\pi^2}\ln\left[\frac{M^2}{\mu^2}\right]\frac{M^2}{F^2}\right), \quad l_4 = l_4^r + \gamma_4\lambda, \quad l_4^r = \frac{\gamma_4}{32\pi^2}\left(\bar{l}_4 + \ln\frac{M^2}{\mu^2}\right), \gamma_4 = 2,\\
&g_A = g + 4d_{16}M^2 + \Delta_g,\\
&\Delta_g = \frac{g\left[4(g^2-2)m_N^2 + (3g^2+2)M^2\right]}{16\pi^2F^2(4m_N^2 - M^2)}A_0[m_N^2] + \frac{g\left[(8g^2+4)m_N^2 - (4g^2+1)M^2\right]}{16\pi^2F^2(4m_N^2 - M^2)}A_0[M^2]\\
&\quad + \frac{gM^2\left[-8(g^2+1)m_N^2 + (3g^2+2)M^2\right]}{16\pi^2F^2(4m_N^2 - M^2)}B_0[m_N^2, m_N^2, M^2] - \frac{g^3m_N^2(4m_N^2 + 3M^2)}{16\pi^2F^2(4m_N^2 - M^2)},
\end{aligned} \tag{23}$$

where μ represents the renormalization scale which we fix at $\mu = m_N$, and λ is a m_π independent infinite renormalization constant [32, 33]. The Passarino-Veltman functions, A_0 and B_0, are adopted from [36] and have the following analytic expressions:

$$\begin{aligned}
A_0[m^2] &= m^2\left(-R_\epsilon + \ln\frac{\mu^2}{m^2}\right),\\
B_0[p^2, m_1^2, m_2^2] &= 1 - R_\epsilon + \ln\left(\frac{\mu^2}{m_2^2}\right)\\
&\quad + \frac{1}{2p^2}\left\{\left[p^2(1+\rho) - R_m\right]\ln\left[\frac{R_m + p^2(1-\rho)}{R_m - \rho^2(1+\rho)}\right]\right.\\
&\quad \left. + \left[\rho^2(1-\rho) - R_m\right]\ln\left[\frac{R_m + p^2(1+\rho)}{R_m - \rho^2(1-\rho)}\right]\right\}
\end{aligned} \tag{24}$$

where $R_\epsilon = -\frac{1}{\epsilon} + \gamma_E - \ln(4\pi) - 1$, with $\gamma_E = -\Gamma'(1)$ denoting the Euler constant; ρ and R_m are defined as follows:

$$\rho = \frac{\sqrt{p^2 - (m_1 + m_2)^2}\sqrt{p^2 - (m_1 - m_2)^2}}{p^2}, \quad R_m = m_2^2 - m_1^2. \tag{25}$$

Using the aforementioned formulas, the resulting dependence relations are visualized in Fig. 2. The following parameter values are adopted in the calculations: $d_{16} = -0.83\,\text{GeV}^{-2}$ [35, 37] and LEC $l_4^r = 0.00373$ is derived through the evolution of its conventional value at renormalization scale $\mu = 0.77$ [38, 39] to $\mu = m_N$. For the three sets of m_N vs. m_π dependence curves presented in the figure, the corresponding c_1 parameters are chosen from Ref. [3] for the $O(p^2)$ order, Ref. [40] for the

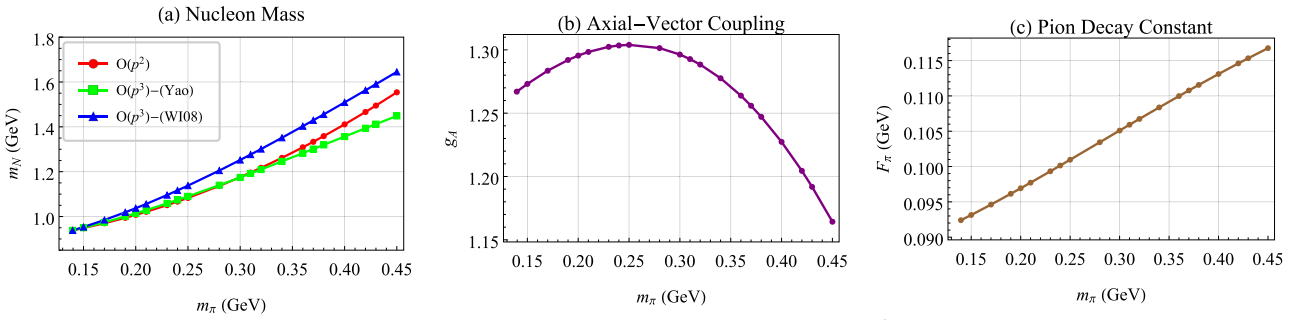

Fig. 2. (color online) Dependencies of the nucleon mass m_N, axial-vector coupling g_A, and pion decay constant F_π on the pion mass m_π.

$O(p^3)-$(Yao) set and Ref. [41, 42] for the $O(p^3)-$(WI08) set, respectively. Since we do not consider explicit $\Delta(1232)$ in the BχPT, we choose the parameter sets in the cases without explicit $\Delta(1232)$ from these references.

By substituting these derived dependence relations into the partial-wave unitary matrix element, we ultimately obtain the trajectory of the $N^*(920)$ resonance as pion mass varies from 0.1396 GeV to 0.45 GeV, which is further extended to 0.60 GeV when considering $O(p^2)$ contributions, since $O(p^2)$ calculation is numerically more stable. Fig. 3 illustrates the evolution of this $N^*(920)$ pole trajectory in the w-plane (where $w=\sqrt{s}$): as pion mass increases, the pole gradually migrates toward the real axis. $O(p^2)$ result shows a more complete picture: the pole ultimately traverses the u-cut (at $m_\pi = 0.526$GeV), thereby entering the adjacent Riemann sheet. Furthermore, the crossing position is consistent with the result calculated via Equation (43) in Ref. [20], which is expressed as:

$$(m_N-m_\pi-w)(m_N+m_\pi-w)\left[m_N(m_N-w)(m_N+w)^2-m_\pi^4\right]=0,$$
$$w=\sqrt{s} \tag{26}$$

For the $O(p^3)$ calculations, more low energy constants are needed compared with $O(p^2)$. We use the results of Fit 1 in Ref. [40](denoted as $O(p^3)-$Yao in Fig. 3):

$$\begin{aligned}
&c_1=-1.22\,\mathrm{GeV}^{-1}, \quad c_2=3.58\,\mathrm{GeV}^{-1},\\
&c_3=-6.04\,\mathrm{GeV}^{-1}, \quad c_4=3.48\,\mathrm{GeV}^{-1}\\
&d_1+d_2=3.25\,\mathrm{GeV}^{-2}, \quad d_3=-2.88\,\mathrm{GeV}^{-2},\\
&d_5=-0.15\,\mathrm{GeV}^{-2}, \quad d_{14}-d_{15}=-6.19\,\mathrm{GeV}^{-2},\\
&d_{18}=-0.47\,\mathrm{GeV}^{-2}
\end{aligned} \tag{27}$$

Using these low energy constants, the corresponding positions of $N^*(920)$ pole are found to be $\sqrt{s}=0.896\pm i0.258$ GeV. Specifically, as the pion mass increases from 0.1396 GeV to 0.45 GeV, the trajectory of $N^*(920)$ is approaching the u-cut as shown in Fig. 3.

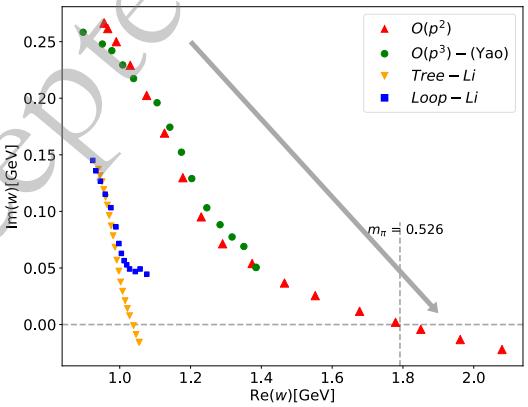

Fig. 3. (color online) Variation of the $N^*(920)$ pole position with the pion mass in the $\mathcal{K}^{(2)}$ and $\mathcal{K}^{(3)}$ amplitudes. The units for the pole positions are in GeV. The results obtained in this work are shown in red upright triangles ($O(p^2)$ tree-level), covering $m_\pi = 0.1396 \sim 0.60$ GeV and green solid circle ($O(p^3)$ one-loop), covering $m_\pi = 0.1396 \sim 0.45$ GeV. The results from Ref. [20] are also displayed in orange upside-down triangles (Tree–Li) and blue squares (Loop–Li), covering the range $m_\pi = 0.138 \sim 0.360$ GeV.

Here, we have not tracked the trajectory for higher m_π to see whether it crosses the u-cut due to three reasons: first, the trajectory evolution is too slow in the loop calculations; second, the fluctuation in the numerical integral calculation becomes significant, and the searches for the pole become difficult and unstable as the pole approaches the real axis; third, since χPT is a perturbative expansion with respect to m_π, it is reasonable to expect that at higher orders the region in which it provides a good approximation would become smaller. Thus, from the $O(p^3)$ result, we are not sure whether the pole will touch the u-cut and move across to the adjacent Riemann sheet for larger m_π.

We also compare our results with those from Ref. [20], which were obtained using the Linear Sigma Model (LσM) with nucleons. While the overall trends of the trajectories are consistent, the rate at which the pole approaches the real axis in the LσM is notably higher at

both tree and one-loop levels. This causes the pole to cross the u-cut at a smaller pion mass in their tree-level calculation. Furthermore, due to the limited applicability range of the LσM, the authors did not extend their one-loop calculation to very large pion masses. Consequently, the pole in the LσM appears to remain on the complex plane without reaching the real axis. In contrast, here, the $O(p^3)$ result shows that the trajectory continues to bend downward toward the real axis with increasing m_π, following a trend similar to the tree-level behavior.

In addition, we also tested another set of parameters [41, 42], referred to as WI08 parameter set, and found that the $O(p^3)$ calculation yields consistent results. The results are shown in Fig. 4 below, and the specific parameters are listed as follows:

$$\begin{aligned}
&c_1 = -1.50\,\mathrm{GeV}^{-1}, \quad c_2 = 3.76\,\mathrm{GeV}^{-1},\\
&c_3 = -6.63\,\mathrm{GeV}^{-1}, \quad c_4 = 3.68\,\mathrm{GeV}^{-1}\\
&d_1 + d_2 = 3.67\,\mathrm{GeV}^{-2}, \quad d_3 = -2.63\,\mathrm{GeV}^{-2},\\
&d_5 = -0.07\,\mathrm{GeV}^{-2}, \quad d_{14} - d_{15} = -6.80\,\mathrm{GeV}^{-2},\\
&d_{18} = -0.50\,\mathrm{GeV}^{-2}.
\end{aligned} \tag{28}$$

In addition to the dependence relations for m_N, g_A and F_π derived from chiral perturbation theory, similar results are also available by some theoretical fits performed on the lattice data. For m_N, we use the ruler approximation in Ref. [43], that is, $m_N = 800\,\mathrm{MeV} + m_\pi$, which is consistent with the lattice QCD results [44, 45] in a large range. For g_A, we use the $O(p^3)$ result in Ref. [46] (Fig. 4.), and for F_π, we use the fit result with strategy 2 (left subfigure in Fig. 4.) in Ref. [47]. Based on these dependence relations, the resulting trajectory of the $N^*(920)$ pole is shown in Fig. 5. It seems that the points where the $N^*(920)$ pole approaches the u-cut from the $O(p^2)$ and $O(p^3)$ chiral perturbation theory calculations tend to converge. However, since there is no guarantee that the pole reaches the u-cut at the same m_π for both $O(p^2)$ and $O(p^3)$ results, this convergence may just be accidental.

As illustrated in this section, the $N^*(920)$ pole trajectory obtained in different approximations and parameter sets are in qualitative agreement with each other.

IV. SUMMARY

In this paper, we have investigated the trajectory of $N^*(920)$ as the pion mass increases within the BχPT framework both at $O(p^2)$ and $O(p^3)$ orders. In BχPT, the functions of the nucleon mass, pion decay constant, and πN axial-vector coupling as a function of the pion mass are obtained self-consistently, provided that the LECs are fixed. In both cases, the $N^*(920)$ moves along a rightward-downward trajectory toward the u-cut on the complex energy plane. At $O(p^2)$ level, the pole will eventually cross the u-cut, entering the adjacent Riemann sheet defined by the u-cut. The result at $O(p^3)$ order shows that the circular cut has marginal effects on the trajectory, and the higher-order contributions slow down the approaching rate of the pole. Furthermore, to test the robustness, we tried three different LEC parameter sets. All three results demonstrate that the $N^*(920)$ moves toward the u-cut. But since the numerical results at $O(p^3)$ become unstable as the pole moves closer to the real axis and the higher order chiral expansion may not be good at larger m_π, we are not sure whether it will meet the u-cut and get across to the adjacent Riemann sheet. The trajectory is also compared with the result in the previous work [20], showing qualitatively consistent behaviors. Our analyses made in

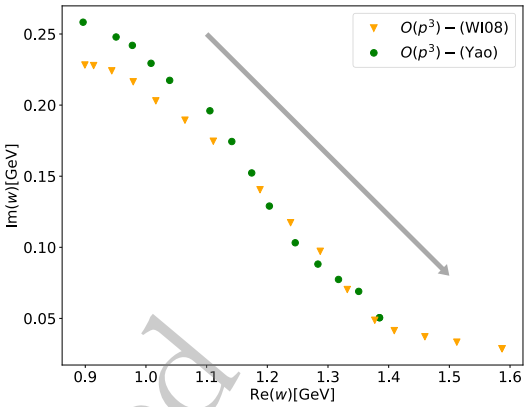

Fig. 4. (color online) m_π dependence of $N^*(920)$ pole from the full $O(p^3)$ amplitude including loop corrections, using parameters from Eq. (31). The previous $O(p^3)$-(Yao) result in Fig. 3 is also displayed for comparison.

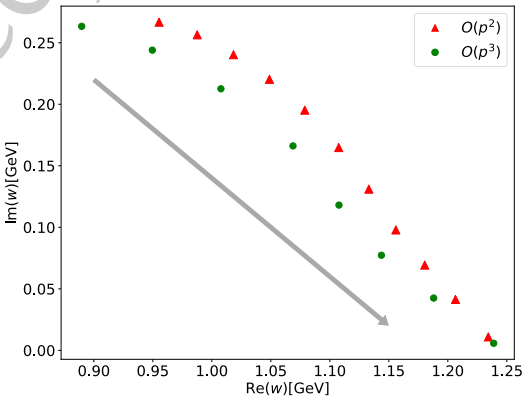

Fig. 5. (color online) The dependence of the $N^*(920)$ pole position on pion mass, as determined from the $\mathcal{K}^{(2)}$ and $\mathcal{K}^{(3)}$ amplitudes (with the dependencies of m_N, g_A, and F_π on m_π taken from lattice–data–based fits). The unit is GeV. The $\mathcal{K}^{(2)}$ results are indicated by red triangles, while the $\mathcal{K}^{(3)}$ results are shown as green circles. The pion mass m_π varies from 0.1396 to 0.44 GeV.

this paper may provide valuable insights for future Lattice studies with unphysical pion masses.

ACKNOWLEDGMENT

We thank Zhi-Hui Guo for helpful discussions.

References

[1] Q.-Z. Li and H.-Q. Zheng, Commun. Theor. Phys. **74**(11), 115203 (2022), arXiv: 2108.03734[nucl-th]
[2] H. Q. Zheng, Z. Y. Zhou, G. Y. Qin, Z. Xiao, J. J. Wang, and N. Wu, Nucl. Phys. A **733**, 235 (2004), arXiv: hep-ph/0310293
[3] Y.-F. Wang, D.-L. Yao, and H.-Q. Zheng, Eur. Phys. J. C **78**(7), 543 (2018), arXiv: 1712.09257[hep-ph]
[4] Y.-F. Wang, D.-L. Yao, and H.-Q. Zheng, Chin. Phys. C **43**(6), 064110 (2019), arXiv: 1811.09748[hep-ph]
[5] Y. Ma, W.-Q. Niu, Y.-F. Wang, and H.-Q. Zheng, Commun. Theor. Phys. **72**(10), 105203 (2020), arXiv: 2002.02351[hep-ph]
[6] Q.-Z. Li, Y. Ma, W.-Q. Niu, Y.-F. Wang, and H.-Q. Zheng, Chin. Phys. C **46**(2), 023104 (2022), arXiv: 2102.00977[nucl-th]
[7] X.-H. Cao, Q.-Z. Li, and H.-Q. Zheng, JHEP **12**, 073 (2022), arXiv: 2207.09743[hep-ph]
[8] M. Hoferichter, J. R. de Elvira, B. Kubis, and U.-G. Meißner, Phys. Lett. B **853**, 138698 (2024), arXiv: 2312.15015[hep-ph]
[9] M. Döring, J. Haidenbauer, M. Mai, and T. Sato, Prog. Part. Nucl. Phys. **146**, 104213 (2026), arXiv: 2505.02745[nucl-th]
[10] Q.-Z. Li, Z. Xiao, and H.-Q. Zheng, *Eur. Phys. J. Spec. Top.* (5, 2025), arXiv: 2505.24674 [hep-ph].
[11] M. Luscher, Nucl. Phys. B **354**, 531 (1991)
[12] K. Rummukainen and S. A. Gottlieb, Nucl. Phys. B **450**, 397 (1995), arXiv: hep-lat/9503028
[13] Z. Fu, Phys. Rev. D **85**, 014506 (2012), arXiv: 1110.0319[hep-lat]
[14] L. Leskovec and S. Prelovsek, Phys. Rev. D **85**, 114507 (2012), arXiv: 1202.2145[hep-lat]
[15] X.-H. Cao, Q.-Z. Li, Z.-H. Guo, and H.-Q. Zheng, Phys. Rev. D **108**(3), 034009 (2023), arXiv: 2303.02596[hep-ph]
[16] X.-H. Cao, F.-K. Guo, Z.-H. Guo, and Q.-Z. Li, Phys. Rev. D **112**, L031503 (2025), arXiv: 2412.03374[hep-ph]
[17] X.-H. Cao, F.-K. Guo, Z.-H. Guo, and Q.-Z. Li, Phys. Rev. D **112**(3), 034042 (2025), arXiv: 2506.10619[hep-ph]
[18] Y.-L. Lyu, Q.-Z. Li, Z. Xiao, and H.-Q. Zheng, Phys. Rev. D **110**(9), 094054 (2024), arXiv: 2405.11313[hep-ph]
[19] Y.-L. Lyu, Q.-Z. Li, Z. Xiao, and H.-Q. Zheng, Phys. Rev. D **109**(9), 094026 (2024), arXiv: 2402.19243[hep-ph]
[20] Q.-Z. Li, Z. Xiao, and H.-Q. Zheng, Chin. Phys. C **49**(12), 123103 (2025), arXiv: 2501.01619[hep-ph]
[21] J. Gasser and H. Leutwyler, Annals Phys. **158**, 142 (1984)
[22] N. Fettes, U.-G. Meißner, M. Mojžiš, and S. Steininger, *Annals Phy.* **283** no. 2, (2000) 273–307. https://www.sciencedirect.com/science/article/pii/S0003491600960597.
[23] S. Weinberg, *Nucl. Phys. B* **363** no. 1, (1991) 3–18. https://www.sciencedirect.com/science/article/pii/055032139190231L.
[24] Y.-H. Chen, D.-L. Yao, and H. Q. Zheng, Phys. Rev. D **87**, 054019 (2013), arXiv: 1212.1893[hep-ph]
[25] S. W. MacDowell, Phys. Rev. **116**, 774 (1959)
[26] J. Kennedy and T. D. Spearman, Phys. Rev. **126**(4), 1596 (1962)
[27] G.-Y. Qin, W. Z. Deng, Z. Xiao, and H. Q. Zheng, Phys. Lett. B **542**, 89 (2002), arXiv: hep-ph/0205214
[28] Z. H. Guo, J. J. Sanz Cillero, and H. Q. Zheng, JHEP **06**, 030 (2007), arXiv: hep-ph/0701232
[29] Z. H. Guo, J. J. Sanz-Cillero, and H. Q. Zheng, Phys. Lett. B **661**, 342 (2008), arXiv: 0710.2163[hep-ph]
[30] D.-L. Yao, L.-Y. Dai, H.-Q. Zheng, and Z.-Y. Zhou, Rept. Prog. Phys. **84**(7), 076201 (2021), arXiv: 2009.13495[hep-ph]
[31] M. Gell-Mann, R. J. Oakes, and B. Renner, Phys. Rev. **175**, 2195 (1968)
[32] J. Gasser, M. Sainio, and A. Švarc, *Nucl. Phys. B* **307** no. 4, (1988) 779–853. https://www.sciencedirect.com/science/article/pii/0550321388901083.
[33] J. Gasser and H. Leutwyler, Annals Phys. **158**, 142 (1984)
[34] X.-L. Gao, Z.-H. Guo, Z. Xiao, and Z.-Y. Zhou, Phys. Rev. D **105**(9), 094002 (2022), arXiv: 2202.03124[hep-ph]
[35] D.-L. Yao, L. Alvarez-Ruso, and M. J. Vicente-Vacas, Physical Review D **96**(11), 116022 (2017)
[36] G. Passarino and M. J. G. Veltman, Nucl. Phys. B **160**, 151 (1979)
[37] J.-M. Chen, Z.-R. Liang, and D.-L. Yao, Front. Phys. (Beijing) **19**(6), 64202 (2024), arXiv: 2403.17743[hep-ph]
[38] J. Bijnens, PoS **CD12**, 002 (2013), arXiv: 1301.6953[hep-ph]
[39] G. Colangelo, J. Gasser, and H. Leutwyler, *Nucl. Phys. B* **603** no. 1–2, (June, 2001) 125–179. http://dx.doi.org/10.1016/S0550-3213(01)00147-X.
[40] D.-L. Yao, D. Siemens, V. Bernard, E. Epelbaum, A. M. Gasparyan, J. Gegelia, H. Krebs, and U.-G. Meißner, JHEP **05**, 038 (2016), arXiv: 1603.03638[hep-ph]
[41] J. M. Alarcon, J. M. Camalich, and J. A. Oller, *PoS* **ConfinementX** (2012) 122, arXiv: 1301.3067 [hep-ph].
[42] J. Alarcón, J. Martin Camalich, and J. Oller, *Annals Phys.* **336** (Sept., 2013) 413–461. http://dx.doi.org/10.1016/j.aop.2013.06.001.
[43] A. Walker-Loud, PoS **LATTICE2013**, 013 (2014), arXiv: 1401.8259[hep-lat]
[44] XQCD Collaboration, M. Gong *et al.*, Phys. Rev. D **88**, 014503 (2013), arXiv: 1304.1194[hep-ph]
[45] M. Hoferichter, J. Ruiz de Elvira, B. Kubis, and U.-G. Meissner, Phys. Rept. **625**, 1 (2016)
[46] F. Alvarado and L. Alvarez-Ruso, Phys. Rev. D **105**(7), 074001 (2022), arXiv: 2112.14076[hep-ph]
[47] M. Niehus, M. Hoferichter, B. Kubis, and J. Ruiz de Elvira, Phys. Rev. Lett. **126**(10), 102002 (2021), arXiv: 2009.04479[hep-ph]